International Journal of Adhesion & Adhesives 30 (2010) 200–207

Contents lists available at ScienceDirect

International Journal of Adhesion & Adhesives

journal homepage: www.elsevier.com/locate/ijadhadh

Facile one-pot synthesis and characterization of maleated hydrocarbon resin tackifier for improved adhesion

K. Dinesh Kumar [a], Andy H. Tsou [b], Anil K. Bhowmick [a,*,1]

[a] Rubber Technology Centre, Indian Institute of Technology, Kharagpur 721302, India
[b] Corporate Strategic Research, ExxonMobil Research and Engineering, Annandale, NJ 08801, USA

ARTICLE INFO

Article history:
Accepted 11 January 2010
Available online 20 January 2010

Keywords:
Novel adhesives
Rubbers
Contact angles
Tack
Tackifier

ABSTRACT

This work reports for the first time the facile method for grafting maleic anhydride (MAH) to solid C5-aliphatic hydrocarbon resin tackifier (HCR). MAH grafting has been carried out thermally (240°C) without using any peroxide. It has been shown that up to 30 wt% of MAH can be conveniently grafted to the HCR via thermal process. Fourier transform infrared spectroscopy (FT-IR) and proton nuclear magnetic resonance (^{1}H-NMR) spectroscopy confirm that the MAH has been appended to the HCR. The effect of varying MAH concentration, reaction time and reaction temperature on the grafting efficiency (GE) has been reported. The grafting degree (wt%) and grafting efficiency (GE) of the maleated (MA-g-HCR) samples have been determined by FT-IR spectroscopy and solvent extraction. The MA-g-HCR samples have been thoroughly characterized by using gel permeation chromatography, differential scanning calorimetry, thermogravimetric analysis, contact angle measurements and X-ray photoelectron spectroscopy. A steady increase in the molecular weight, glass transition temperature, melting point and maximum degradation temperature of the HCR tackifier has been observed with the increasing weight percentage of MAH grafting. It has been shown that the polar component of the surface energy of HCR resin can be increased up to $9 \pm 3\,mN\,m^{-1}$ by grafting 30 wt% of MAH.

1. Introduction

Tackifiers are vital compounding ingredients used in adhesive and rubber industry to improve tack and tack retention properties. Three major types of tackifiers are: hydrocarbon resins, rosin and its derivatives and phenol–formaldehyde resins [1–3]. Tackifying resins typically have a molecular weight of ca 2000 or less [2]. Hydrocarbon resin tackifiers are low molecular weight polymers derived from crude monomer streams [1–4]. Hydrocarbon resin streams obtained from petroleum based feed stocks can be classified as aliphatic (C5), aromatic (C9) and dicyclopentadiene (DCPD) or mixtures of these. Polymerization of these streams is carried out using a Lewis acid catalyst or by a free-radical process using heat and pressure [1]. Because of the variety of feed streams available and the various polymerization techniques employed, a wide variety of hydrocarbon resins is available with broad range of properties. In addition, hydrogenated hydrocarbon resin tackifiers show good stability towards oxidation due to their mostly saturated backbone. It is this diversity that makes hydrocarbon resins more useful in adhesive and tire industry [1–4].

In adhesive industries, hydrocarbon resins are used as tackifiers in pressure sensitive [5] and hot melt adhesives [6]. The amounts of the hydrocarbon resin used in the adhesive formulations are quite large, sometimes equaling the weight of the base polymers in the formulations. On the other hand, tire industries use 5–15 parts of hydrocarbon resin per 100 parts of elastomer in rubber compounding to increase the autohesive tack of synthetic elastomers [7–10].

However, the inherent non-polar nature of the hydrocarbon resins restricts their utility in applications where strong polar interactions are required between the joining surfaces. In such cases, the polar tackifiers like rosins or phenolic resins are extensively used. Because rosin is an acidic material, its acid functionality is utilized in many commercial applications like: adhesives, surface coatings and as compounding ingredients for synthetic elastomers [1]. However, there are two major disadvantages of rosin tackifiers, namely their low aging stability, and the inadequate coating/processing properties of their aqueous dispersions (related to its water sensitivity) [1]. On the other hand, phenolic resin tackifiers are very expensive. Moreover, polar tackifier will not be effective in improving the tack of fully non-polar elastomers due to the existence of wide difference in the

* Corresponding author. Tel.: +91 3222 283180; fax: +91 3222 220312.
E-mail address: anilkb@rtc.iitkgp.ernet.in (A.K. Bhowmick).
[1] Present address: Indian Institute of Technology, Patna 800013, India.

0143-7496/$ - see front matter © 2010 Elsevier Ltd. All rights reserved.
doi:10.1016/j.ijadhadh.2010.01.001

compatibility between the elastomer and the tackifier [11]. It is particularly important in view of our recent work on nearly non-polar brominated isobutylene-co-p-methylstyrene (BIMS) rubber where phenolic resin tackifier has been found to be not so useful in improving the tack property of the BIMS elastomer [11]. Therefore, in some adhesive formulations, blend of hydrocarbon resin (HCR) and polar tackifiers are used to achieve a reasonable balance between the compatibility and the adhesive performance [1]. But using two different tackifiers of different nature in the adhesive formulation can have some negative influence on the adhesive performance. Also, this will increase the compounding time and cost of the adhesive. Therefore, a novel tackifier, that is relatively inexpensive and which provides excellent adhesive and cohesive strength to the adhesive through their tailor-made chemical structure have been sought.

In this work, the above mentioned objective has been attained by synthesizing polar HCR tackifier via reacting maleic anhydride (MAH) with the HCR tackifier. In literature, there are few patented works that examine the different modification procedures of HCR tackifiers [12]. However, to our knowledge, there are no reports in open literature which describe the polar modification of mostly saturated solid C5-aliphatic HCR tackifier. This paper reports the facile method for grafting maleic anhydride onto the solid C5-aliphatic HCR tackifier. The extent of grafting has been varied from 5 to 30 wt% of MAH. It has been shown that MAH can be easily appended to the HCR tackifier by a simple thermal process in the absence of any initiator or catalyst. The maleated hydrocarbon resin tackifier (MA-g-HCR) has been thoroughly characterized by different techniques to understand the efficacy of this modification technique. The effect of polar modification on the glass transition temperature (T_g), molecular weight and thermal stability of the HCR has been shown. This maleated hydrocarbon resin tackifier can be used as a potential alternative for rosin and phenolic resin tackifiers.

2. Experimental

2.1. Materials

Escorez™ hydrocarbon resin (C5-aliphatic hydrocarbon resin tackifier; softening point: 96–104 °C; glass transition temperature 50 °C; and M_w=2220) was supplied by the ExxonMobil Chemical Company, Baytown, TX, USA and maleic anhydride (laboratory grade) was procured from E. Merck, Mumbai, India.

2.2. Synthesis of maleated hydrocarbon resin tackifier (MA-g-HCR)

MAH grafting was carried out thermally at high temperature in the absence of initiators. 10 g of HCR were placed in a 500 mL three-necked round bottom flask fitted with a thermometer and condenser. Required amount of MAH was added to the three-necked round bottom flask. The HCR and MAH mixture was heated to 235–240 °C for 2 h under nitrogen. Once the reaction temperature was reached, the reaction was continued for additional 2 h under nitrogen. The stirring of the mixtures was accomplished by using a magnetic paddle at 750 rpm. The amount of MAH was varied from 5 to 30 weight percent on total mixture. Finally, the MA-g-HCR was decanted from the three-necked round bottom flask into an aluminum pan. The details of the composition of the samples are enlisted in Table 1.

2.3. Determination of grafting degree (GD) and grafting efficiency (GE) of MAH through the Soxhlet extraction

The MA-g-HCR samples placed on filter paper were placed in a Soxhlet apparatus for extraction. For complete removal of unreacted MAH, each extraction was carried out for 24 h, using methanol as the extracting medium. After extraction, the samples on filter paper were dried under vacuum for 72 h at 70 °C till they showed no weight variation (W_g). The GD and GE were calculated from Eqs. (1) and (2) respectively [13].

$$GD = [(W_g - W_0)/W_0] \times 100 \quad (1)$$

$$GE = [(W_g - W_0)/W_m] \times 100 \quad (2)$$

where W_g, weight of grafted HCR; W_0, weight of HCR before grafting and W_m, weight of the maleic anhydride monomer added.

2.4. Fourier transform infrared spectroscopic (FT-IR) studies

The infrared spectra of the HCR and Soxhlet extracted MA-g-HCR samples were recorded with a Perkin-Elmer FT-IR spectrophotometer (Shelton, CT, USA) at room temperature (25 °C). In order to obtain the base spectra of the samples, FT-IR absorbance spectra were obtained from sample/KBr pellets. A milligram of the finely ground sample was mixed with 100 mg of dried KBr powder within a sample set. A pressure of 69–103 MPa was applied for 2 min to yield a disk. All samples were scanned from 4000 to 400 cm^{-1} with a resolution of 4 cm^{-1}. All spectra were reported after an average of 32 scans.

2.5. Nuclear magnetic resonance (^{1}H-NMR) spectroscopy

Proton nuclear magnetic resonance (^{1}H-NMR) spectra were recorded in a 200-MHz Bruker NMR spectrophotometer (Billerica, MA, USA). All scans were taken after dissolution of the samples in $CDCl_3$.

2.6. Gel permeation chromatographic (GPC) studies

The molecular weights of the samples were determined by size exclusion chromatography (SEC) at ambient temperature using a Viscotek Gel Permeation Chromatography (Viscotek, Houston, TX, USA) equipped with a VE 1122 solvent delivery system, a VE 3580 RI detector, and two ViscoGEL mixed bed columns (17392-GMHHRM), which were preceded by a guard column that protects

Table 1
Composition of samples.

Sample number	Designation	Hydrocarbon resin (HCR) (grams)	Maleic anhydride (MAH) in phr[a]
1.	E1102	100	0
2.	5ME1102	100	5
3.	10ME1102	100	10
4.	20ME1102	100	20
5.	30ME1102	100	30

[a] phr—parts per 100 g of hydrocarbon resin (HCR).

the main bank of the GPC column from adverse conditions. Data analysis was collected using OmniSEC 4.2 software. THF was used as the eluent at a flow rate of 1.0 ml/min and calibration was carried out using low polydispersity polystyrene standards.

2.7. Glass transition temperature (T_g)

The T_g of samples was measured by DSC (DSC Q 100 from TA Instruments, New Castle, DE, USA), in the temperature range 0–150 °C at a heating rate of 10 °C/min. Dry nitrogen gas was purged into the DSC cell with a flow rate of 50 mL/min. Of about 5–10 mg sample were encapsulated in standard aluminum pans. The scanning runs consisted of heating from room temperature to 150 °C at 10 °C/min, cooling from 150 to 0 °C by quenching, and then heating to 150 °C again at a rate of 10 °C/min. The results of the second run were used for this study.

2.8. Capillary melting point temperature

Very small quantity of the sample was placed on a watch glass. The solid sample was grinded to powder. The grinded sample was gathered into a small pile using spatula. One end of the capillary tube was sealed and other end was kept open to load the sample. The open end of melting point capillary tube was plunged several times into the pile to a depth of about 1 mm. The capillary tube was then inverted and the sealed end was tapped on the bench to encourage the solid to drop to the bottom. The height of sample in the capillary tube was not more than 2–3 mm. The capillary tube filled with sample was tied with a thermometer using a metal wire and immersed in a sulphuric acid bath. The acid bath was heated in a preprogrammed way at a ramp rate of 2 °C/min from 50 to 150 °C. The temperature at which the sample changed into full liquid state was observed and recorded as the capillary melting point of the resin. Each capillary melting point value quoted is the mean of at least three measurements with a maximum error of ± 5 °C.

2.9. Thermogravimetric analysis

Thermogravimetric analysis was done using Perkin-Elmer Instrument, Diamond TG-DTA (Waltham, MA, USA). The samples (3–5 mg) were heated from ambient temperature to 800 °C in the furnace of the instrument under oxygen atmosphere at 100 ml/min and at a heating rate of 20 °C/min, and the data of weight loss vs. temperature were recorded. The analysis of the thermogravimetric (TG) and derivative thermogravimetric (DTG) curves was done and the onset temperature, weight loss at major degradation steps and temperature corresponding to the maximum value in the derivative thermogram were recorded. The temperature at which maximum degradation took place is denoted as T_{max} and onset temperature of degradation is denoted as T_i. The error in the measurement was ± 1 °C.

2.10. Surface analysis

2.10.1. Contact angle measurements

The samples for contact angle measurement were prepared by following a procedure given by Comyn [14]. About 5 g of HCR and MA-g-HCR samples were placed on aluminum foil and heated in an oven at 200 °C for 10 min. The molten resin samples were removed and allowed to spread by a glass rod on a glass Petri dish and then heating again in the oven at 200 °C for 5 min, and then the samples were removed and allowed to cool. This produced a perfect flat surface for contact angle measurements. The values of the dispersion, γ_S^D, and polar, γ_S^P, components of surface energy for the HCR and MA-g-HCR samples were obtained using contact angle meter Kernco, Model G-II from Kernco Instruments (EI Paso, TX). The sessile drop method employing 2 μl drops of different probe liquids were applied for contact angle measurements. The liquids used for the contact angle measurements were triply distilled water, and special grades of ethylene glycol, formamide and dimethylsulfoxide all obtained from the Lancaster Synthesis (Morecambe, England). Each contact angle value quoted is the mean of at least five measurements with a maximum error in θ of $\pm 1^\circ$. All investigations were carried in a vapor saturated air at 23 °C in a closed sample box. The advancing contact angle value of probe liquids on the sample at 1 min was observed in all cases.

2.10.2. X-ray photoelectron spectroscopy (XPS) measurements

X-ray photoelectron spectroscopy (XPS) measurements were recorded in an ESCA-3 Mark II spectrometer (VG Scientific Ltd., England) using AlKα radiation (1486.6 eV). Binding energies were calibrated with respect to C (1 s) at 285 eV with a precision of 0.2 eV. For analysis, the samples were made into 0.5 mm thick, 8 mm diameter pellets and placed into an ultra high vacuum chamber at 10^{-9} Torr. The data analysis was done considering the sensitivity factors of each element present.

3. Results and discussion

3.1. Infrared spectroscopic analysis of MA-g-HCR

Fig. 1 shows the FT-IR spectrum of neat HCR (E1102). The peak designations for HCR are listed in Table 2. The FT-IR spectra of the samples 5ME1102, 10ME110, 20ME1102 and 30 ME1102 are given as inset of Fig. 1. On comparing the FT-IR spectra of HCR and MA-g-HCR samples (see inset of Fig. 1), the asymmetric and symmetric carbonyl vibrations at 1862 and 1780 cm^{-1} are observed for the grafted MAH [15–18] in the MA-g-HCR samples besides the inherent vibrations of HCR. Moreover, the intensity of these bands increases gradually with the increase in the concentration of MAH. Also, there is a strong band at 1710 cm^{-1} for the samples 20ME1102 and 30ME1102 due to the carbonyl (C=O) group in COOH [18]. These bands indicate that MAH has been grafted onto HCR. The intensity ratios (C1) of the absorbance peak of C=O at 1780 cm^{-1} and a reference peak of

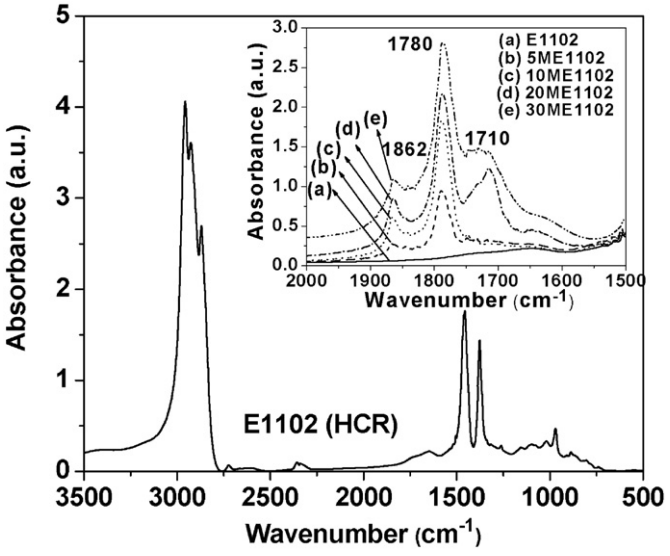

Fig. 1. FT-IR spectrum of E1102 and (inset) FT-IR spectra of E1102, 5ME1102, 10ME1102, 20ME1102 and 30ME1102 in the range 2000–1500 cm^{-1}.

Table 2.
IR bands assignment for E1102.

Serial number	Frequency (cm^{-1})	Vibration
1.	2876–2925	C–H stretching
2.	1458	C–C stretching (alkyl groups)
3.	1376	C–C stretching vibrations of methyl, ethyl, n-propyl, or isopropyl group
4.	970	C–H bending vibrations of n-propyl, isopropyl group or cycloalkane

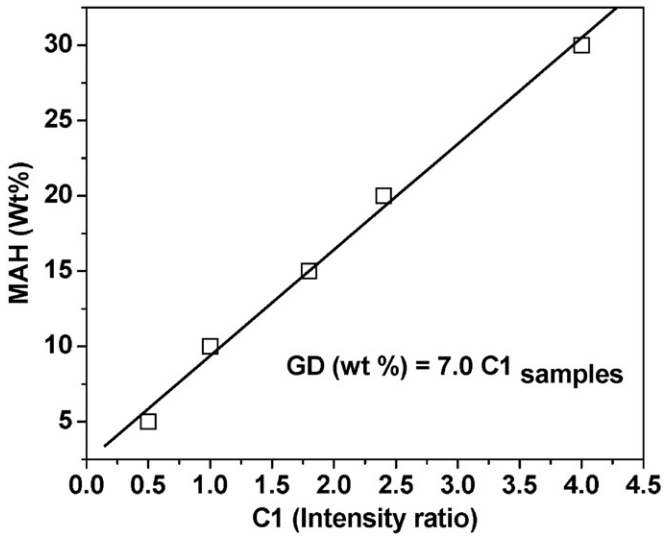

Fig. 2. Calibration curve for FT-IR spectroscopy analysis.

C–C at 1376 cm^{-1}, have been calculated. Calibration curve for FT-IR analysis (Fig. 2) has been established using a series of quantitatively prepared mixtures of HCR and MAH in various compositions. Good correlation among the data has been achieved and the linear relationship is used as the calibration curve. GD (wt%) has been calculated using Eq. (3):

$$\text{GD (wt\%)} = 7.0\ C1_{\text{Samples}} \quad (3)$$

where $C1_{\text{Samples}}$ is the C1 of MA-g-HCR samples.

Qi et al. [16] used a similar technique for estimating the GD of MAH in maleated acrylonitrile–butadiene–styrene (ABS) terpolymer.

Fig. 3 compares the GD calculated from Eqs. (1) and (3). The GD increases steadily with the increasing concentration of MAH. It should be noted that there is good correspondence between the GD estimated from FT-IR spectroscopy and solvent extraction technique. Furthermore, the GE has been calculated from Eq. (2) and the results are plotted in Fig. 3. At all concentrations of MAH, the GE is almost close to 90%, indicating extended degree of reaction between MAH and HCR.

In order to further confirm the grafting of MAH onto the HCR, the ^{1}H-NMR spectra of HCR and 10ME1102 samples are shown in Fig. 4. The ^{1}H-NMR spectra of HCR show broad peaks at 0.85, 1.25 and 1.58 ppm which are assigned to the CH_3 and CH_2 groups in the HCR. Furthermore, the peaks at 5.1 and 5.3 ppm indicate the presence of CH and CH_2 (olefinic groups) in the HCR. On comparing the ^{1}H-NMR spectra of HCR and 10ME1102, a new peak at 3.7 ppm is observed for the MA-g-HCR sample (inset of Fig. 4) besides the expected signals for the HCR. The peak at 3.7 ppm could be assigned to the hydrogen proton on the anhydride ring [16–18]. From the results of FT-IR and ^{1}H-NMR

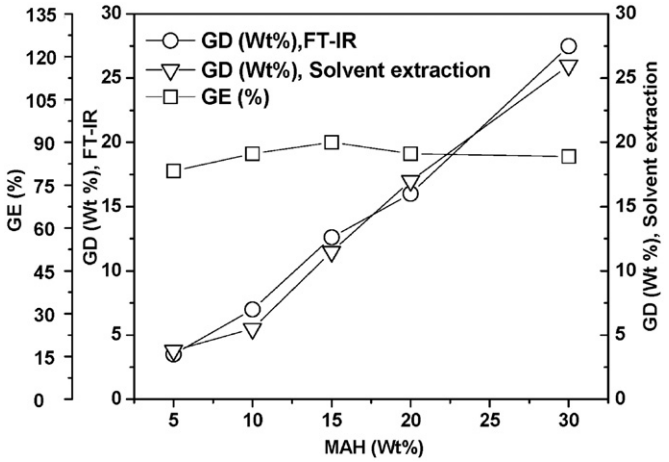

Fig. 3. Variation of GD (from FT-IR spectroscopy), GD (from solvent extraction) and GE with MAH (wt%).

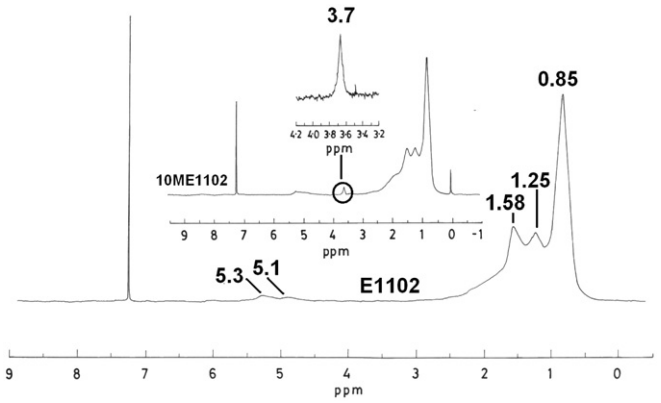

Fig. 4. ^{1}H-NMR spectra of samples E1102 and 10ME1102.

spectra, we can conclude that MAH has been successfully grafted onto the HCR tackifier. Here, the plausible grafting reaction involves initiation to form macroradicals by abstraction of hydrogen atoms from the HCR chain by the initiator radicals (generated at high reaction temperature), and addition of unsaturated monomer (MAH) to the macroradicals. Hasenbein et al. [19] have proposed a similar grafting reaction between MAH and homopolymer or copolymer of ethylene at very high temperatures ($>210\,^{\circ}C$) in the absence of peroxide. Derouet et al. [20] have also suggested a similar grafting reaction between liquid natural rubber and MAH at higher temperatures in the absence of peroxide.

3.2. Effect of reaction parameters on GE

3.2.1. Effect of reaction temperature on GE

To understand the effect of reaction temperature on the GE (from Eq. 2), the grafting reactions have been carried out at 160, 200, 240 and 280 °C. Fig. 5 shows the effect of temperature on the GE for the sample 20ME1102. It is found that the GE increases with the increasing of temperature up to 240 °C. This can be anticipated because the number of free radicals generated and their mobility will be more at high temperatures [16]. Also, there is good reduction in the melt viscosity at higher temperatures, which will facilitate the reaction between the MAH monomer and the HCR and hence the GE is higher. The slight reduction in the GE at 280 °C can be attributed to various reasons. Although the rate of

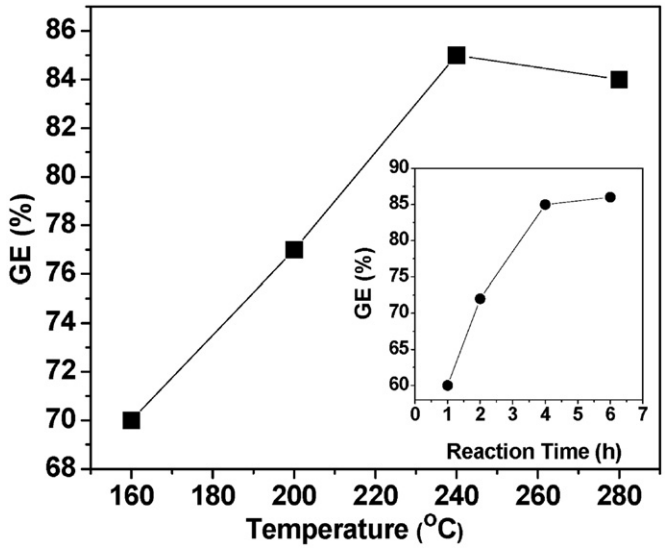

Fig. 5. Effect of reaction temperature on GE and (inset) effect of reaction time on GE.

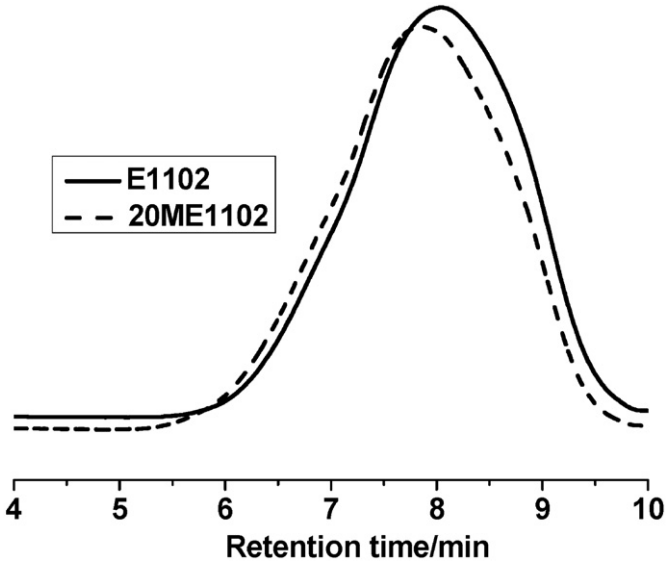

Fig. 6. GPC traces of E1102 (solid line) and 20ME1102 (dashed line).

Table 3
Molecular weight values of samples from GPC.

Sample number	Designation	M_w	M_v
1.	E1102	2220	2024
2.	5ME1102	2335	2122
3.	10ME1102	2361	2204
4.	20ME1102	2466	2290
5.	30ME1102	2610	2413

the reactions will increase, there will be many side reactions. Also, the probability of degradation of the HCR will increase with temperature. Homopolymerization of MAH cannot be ruled out. [16].

3.2.2. *Effect of reaction time on GE*

To understand the effect of reaction time on the GE (from Eq. 2) of sample 20ME1102, the grafting reactions have been carried out for 1, 2, 4 and 6 h at the optimized reaction temperature (240 °C). Inset of Fig. 5 shows the effect of reaction time on the GE for the sample 20ME1102. The GE steadily increases with the increase in reaction time and finally levels of at 4 h.

3.3. *Molecular weight studies through gel permeation chromatography (GPC)*

The HCR and the MA-g-HCR samples are characterized by weight average molecular weight (M_w) and viscosity average molecular weight (M_v) obtained from GPC. M_w and M_v of the HCR increase gradually with increasing weight percentage of grafting (Table 3). Furthermore, there is a shift in the GPC trace after grafting MAH onto the HCR (Fig. 6) that may evidence for the grafting of MAH. The increase in molecular weight of the HCR with the addition of MAH can be ascribed to the presence of MAH groups in the HCR after the grafting reaction.

3.4. *Glass transition temperature (T_g) and melting point (T_m)*

Fig. 7 shows the DSC curves of HCR and MA-g-HCR samples. DSC data show that the presence of maleic anhydride groups in

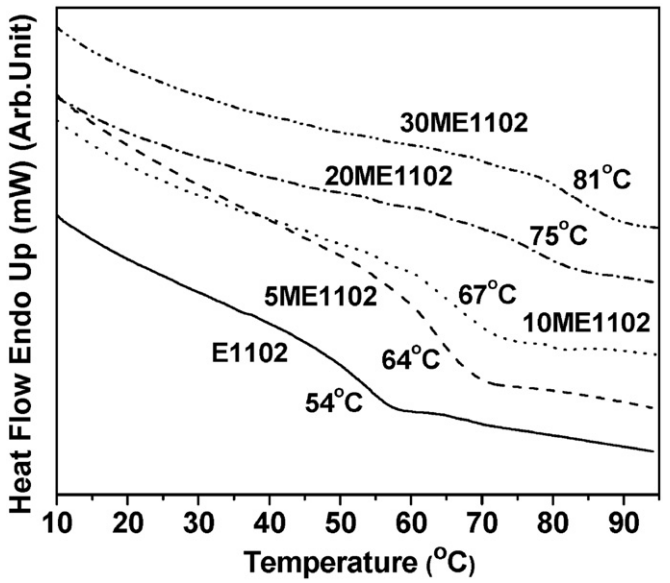

Fig. 7. DSC traces of E1102 and MA-g-HCR samples.

the MA-g-HCR samples affects the glass transition temperature of the HCR. An increase of T_g is observed for maleated products when compared to the unmodified precursor (see Table 4). In accordance with the literature [21], increasing polar functionality with respect to the alkyl nature of any polymer increase intermolecular interactions, reducing mobility in the chains and therefore increasing the glass transition temperature. The increase in the glass transition temperature of HCR with increasing weight percentage of grafting is indicative of an increase of polar anhydride groups in the HCR. A similar increase in the capillary melting point temperature is observed for MA-g-HCR samples when compared to the HCR (see Table 4), due to the similar reason stated above.

3.5. *Thermal stability studies*

The thermogravimetry (TG) and differential thermogravimetric (DTG) plots for HCR and MA-g-HCR samples are compared

Table 4
Glass transition temperature (T_g) and capillary melting point temperature (T_m) of HCR and MA-g-HCR samples.

Sample number	Designation	Glass transition temperature (T_g) (°C)	Capillary melting point temperature (°C)
1.	E1102	54	105–115
2.	5ME1102	64	115–125
3.	10ME1102	67	120–130
4.	20ME1102	75	125–135
5.	30ME1102	81	135–145

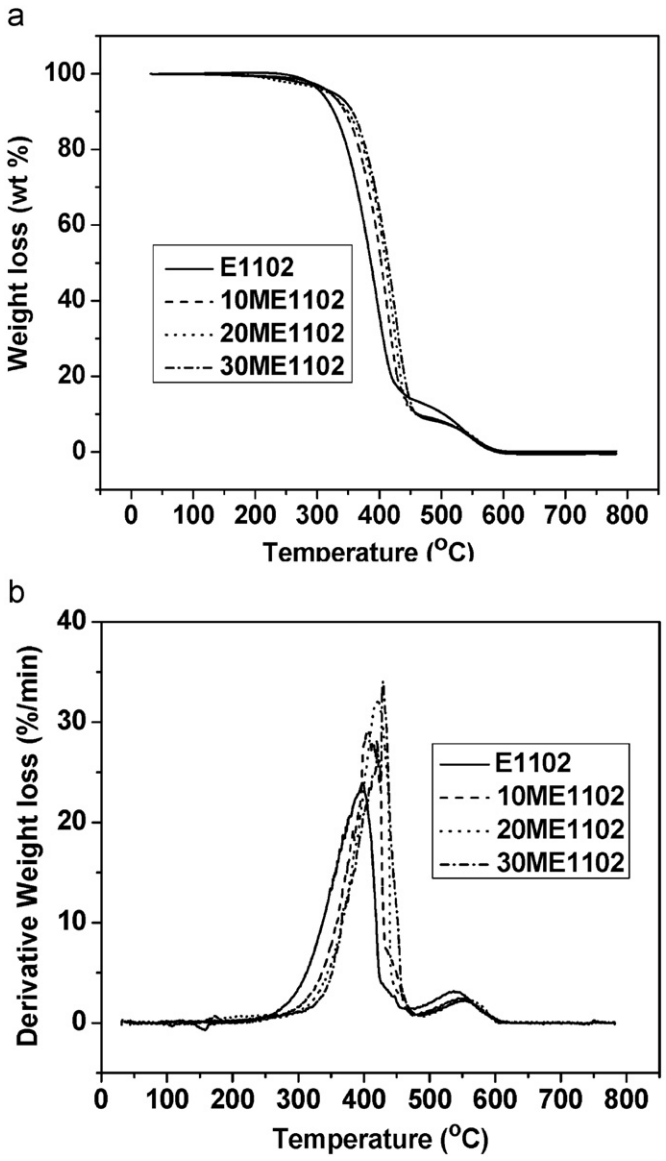

Fig. 8. (a) TGA plots of HCR and MA-g-HCR samples. (b) DTG plots of HCR and MA-g-HCR samples.

in Fig. 8a and b respectively. The temperatures corresponding to the onset of degradation (T_i) and maximum degradation (T_{max}) for these samples are reported in Table 5. The thermal stability of HCR significantly increases with increase in addition of MAH groups to the hydrocarbon resin chains. In the MA-g-HCR, the MAH will act as a physical barrier, thus reducing the oxygen diffusion towards the bulk and hindering the exit of the volatile

Table 5
Onset of degradation (T_i) and maximum degradation (T_{max}) temperature for HCR and MA-g-HCR samples.

Sample number	Designation	T_{onset}	T_{max}
1.	E1102	340	398
2.	10ME1102	366	410
3.	20ME1102	377	422
4.	30ME1102	377	430

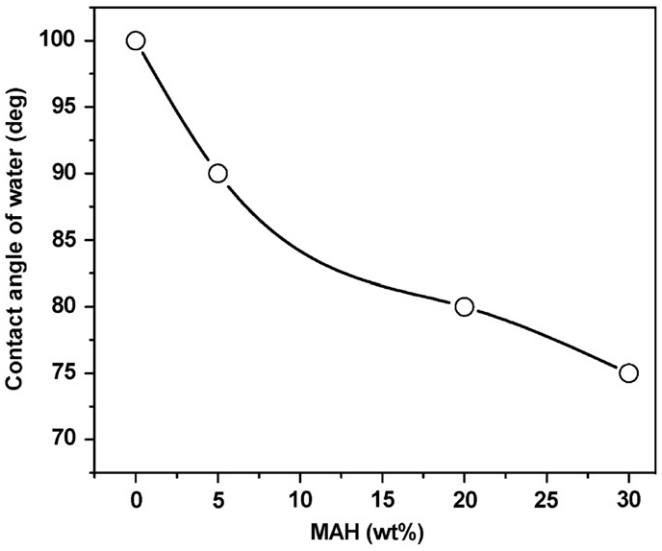

Fig. 9. Contact angle of water on MA-g-HCR vs. percentage of the grafted MAH.

degradation gases from the HCR, just like the effect of fillers [22]. Therefore, the thermal stability of HCR significantly improves in O_2 atmosphere with the addition of MAH.

3.6. Surface properties

3.6.1. Hydrophilicity and surface energy

3.6.1.1. Hydrophilicity. The measurement of the hydrophilicity can be estimated from water contact angle values. The dependence of the water contact angle vs. content of grafted MAH in the MA-g-HCR is given in Fig. 9. The water contact angle on the nongrafted hydrophobic HCR surface is very high and reaches the value of 100°. Since MA-g-HCR is more hydrophilic than HCR, the value of contact angle of water decreases nonlinearly with the increasing concentration of MAH. This indicates that the increase in concentration of MAH imparts hydrophilicity to the HCR. A

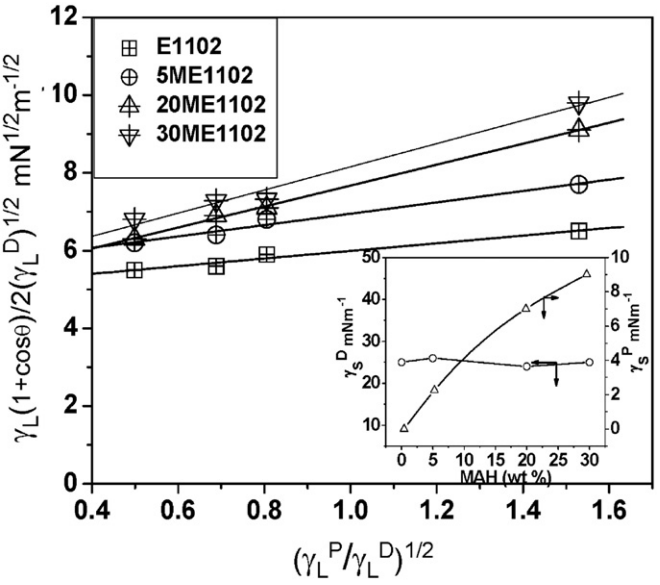

Fig. 10. Plot based on Eq. (5) for contact angle liquids against samples E1102, 5ME1102, 20ME1102 and 30ME1102 and (inset). Experimental dispersion, γ_S^D, and polar, γ_S^P, component values of HCR and MA-g-HCR samples.

similar increase in the hydrophilicity of various other non-polar polymers by grafting MAH is shown in the literature [23–25].

3.6.1.2. Surface energy. By applying the Owens–Wendt approach [26–28], both the polar and dispersion components of the surface free energies of the modified and unmodified samples have been calculated using Eq. (4):

$$\gamma_L(1+\cos\theta) = 2\sqrt{\gamma_S^D\gamma_L^D} + 2\sqrt{\gamma_S^P\gamma_L^P} \quad (4)$$

The above equation can be conveniently rewritten as:

$$\frac{\gamma_L(1+\cos\theta)}{2(\gamma_L^D)^{1/2}} = (\gamma_S^P)^{1/2}\frac{(\gamma_L^P)^{1/2}}{(\gamma_L^D)^{1/2}} + (\gamma_S^D)^{1/2} \quad (5)$$

If the left-hand side of Eq. (5) is plotted against $((\gamma_L^P)^{1/2}/((\gamma_L^D)^{1/2}))$, the graph should be linear with intercept $(\gamma_S^D)^{1/2}$ and slope$(\gamma_S^P)^{1/2}$. Plots of this type for samples E1102, 5ME1102, 20ME1102 and 30ME1102 are shown in Fig. 10. Comyn has used the above procedure to calculate the surface energy of pentaerythritol rosin ester tackifier [14]. The surface energy value of E1102 obtained from it by linear regression analysis is about 25 mN m^{-1}. Since HCR is a fully non-polar material, its surface energy value is obviously low as reported in the literature for other non-polar polymers like ethylene propylene diene polymethylene elastomer and butyl rubber [29–31]. Inset of Fig. 10 shows the variation of polar and dispersion components of the surface free energy of the samples with MAH weight percentage. Comparing these values (see inset of Fig. 10), it can be seen that, in particular, it is the polar component that increases with increase in addition of MAH groups to the hydrocarbon resin chains. The dispersion component remains almost constant for all the samples. Therefore, the MAH polar groups in HCR have a contribution mainly to polar component of the surface energy of MA-g-HCR. It is also clearly seen that the higher the MAH concentration, the higher the surface polarity. The values of surface parameters for the probe liquids (measured at 25 °C) used are shown in Table 6 [14,29,32].

3.6.2. X-ray photoelectron spectroscopy (XPS) studies

From the X-ray photoelectron spectra, the elemental concentrations (C, O) have been determined for samples HCR (E1102) and 10ME1102 and the results are presented in Table 7. It is found that the unmodified E1102 also contains some elemental oxygen, though not detected in FT-IR and ^{1}H-NMR spectroscopy. This can be generally ascribed to the surface oxidation of HCR during processing or storage. However, as a result of grafting MAH (10ME1102), the oxygen content increases due to the formation of carbonyl and carboxylic groups as confirmed from the FT-IR and ^{1}H-NMR studies. This also provided evidence for the grafting MAH onto the HCR. For sample E1102, the C_{1s} peak appears at 284.6 eV binding energy due to the presence of C–C or C–H groups in the HCR and another small peak appears at 286.8 eV binding energy, which corresponds to the C–O groups [14,33,34] arising from the surface oxidation of the HCR. Besides the expected peaks of HCR, two more additional peaks are observed for sample 10ME1102 at 288.1 eV and 289.2 eV binding energy due to the presence of C=O and COO– groups [14,33,34] arising from the grafted MAH.

Table 6
Literature data on contact angle probe liquids measured at 25 °C.

Serial number	Liquids	γ_L^D (mN m^{-1})	γ_L^P (mN m^{-1})	Ref.
1.	Water	21.8	51.0	[14]
2.	Ethylene glycol	29.3	19.0	[32]
3.	Formamide	39.5	18.7	[29]
4.	Dimethyl sulfoxide	34.8	8.6	[32]

Table 7
C and O elemental concentrations in HCR and MA-g-HCR samples.

Sample number	Designation	Element	Concentration (in %)
1.	E1102	C_{1s}	97.7
2.	E1102	O_{1s}	2.3
3.	10ME1102	C_{1s}	88.5
4.	10ME1102	O_{1s}	11.5

4. Conclusions

The MA-g-HCR has been successfully synthesized by thermal process (at 240 °C) in the absence of any initiator, and very high grafting degree (GD wt%) is obtained. The effects of various reaction conditions on the grafting degree have also been studied. The important findings are summarized below:

(1) The FT-IR spectra and ^{1}H-NMR spectra confirm the grafting of MAH onto HCR.
(2) In the graft polymerization of MAH onto HCR, the grafting degree increases with increasing concentration of MAH even at 30 wt% of MAH concentration.
(3) At all concentrations of MAH, the grafting efficiency is almost close to 90%.
(4) From the gel permeation chromatographic (GPC) studies, it is shown that the molecular weight of the HCR tackifier steadily increases with the increasing concentration of MAH, which clearly supports the reaction between the MAH and HCR.
(5) An increase of glass transition temperature (T_g) and capillary melting point temperature is observed for maleated products when compared to the unmodified precursor, which is ascribed to the increase in intermolecular interaction in the maleated species, reducing mobility in the chains and therefore increasing the glass transition temperature.
(6) It is observed that the thermal stability of HCR significantly increases with increase in addition of MAH groups to the

hydrocarbon resin chains. MAH acts as a physical barrier, thus reducing oxygen diffusion towards the bulk and hindering the exit of the volatile degradation gases from the HCR.

(7) The grafting of MAH onto the HCR increases the polar component of the surface tension of HCR up to $9 \pm 3\,\mathrm{mN\,m^{-1}}$ at 30 wt% of MAH concentration.

(8) X-ray photoelectron spectroscopy studies further substantiate the grafting of MAH to the HCR.

Acknowledgement

The authors are thankful to The ExxonMobil Chemical Co., USA, and ExxonMobil Chemical India Pvt. Ltd. for sponsoring the project and according permission to publish the results.

References

[1] Schaldeman JA. Tackifier resins. In: Satas D, editor. Handbook of pressure sensitive adhesive technology. New York: Van Nostrand Reinhold; 1989. p. 353–69.
[2] Powers PG. Resins used in rubber. Rubber Chem Technol 1991;36:1542–70.
[3] Aubrey DW. The nature and action of tackifier resins. Rubber Chem Technol 1988;61:448–69.
[4] Duddey JE. Resins. In: Rodgers MB, editor. Rubber compounding: chemistry and applications. New York: Marcel Dekker; 2004. p. 417–56.
[5] Watson C, Satas D. Hot melt application. In: Satas D, editor. Handbook of pressure sensitive adhesive technology. New York: Van Nostrand Reinhold; 1989. p. 558–73.
[6] Eastman EF, Fullhart L. Polyolefin and ethylene copolymer-based hot melt adhesives. In: Skeist I, editor. Handbook of adhesives, 2nd ed.. New York: Van Nostrand Reinhold; 1990. p. 408–23.
[7] Hamed GR. Tack and green strength of elastomeric materials. Rubber Chem Technol 1981;54:576–95.
[8] Skewis JD. Measurement of rubber tack. Rubber Chem Technol 1965;38: 689–99.
[9] Rhee CK, Andries JC. Factors which influence autohesion of elastomers. Rubber Chem Technol 1981;54:101–14.
[10] Hamed GR, Magnus FL. Role of phenolic tackifiers in polyisoprene rubber. Rubber Chem Technol 1991;64:65–73.
[11] Kumar KD, Tsou AH, Bhowmick AK. Influence of aging on autohesive tack of brominated isobutylene-co-p-methylstyrene (BIMS) rubber in the presence of phenolic resin tackifier. J Adhes 2008;84:764–87.
[12] Theelen MH. (Eastman Chemical Resins Inc.). US Patent 6, 372, 851 B1, April 16, 2002.
[13] Biswas A, Bandyopadhyay A, Singha NK, Bhowmick AK. Chemical modification of metallocene-based polyethylene–octene elastomer through solution grafting of acrylic acid and its effect on the physico-mechanical properties. J Appl Polym Sci 2007;105:3409–17.
[14] Comyn J. Surface characterization of pentaerythritol rosin ester. Int J Adhes Adhes 1995;15:9–14.
[15] Mitov Z, Velichkova R. Modification of styrene–isoprene block copolymers—3. Addition of maleic anhydride—mechanism. Eur Polym J 1993;29:597–601.
[16] Qi R, Chen Z, Zhou C. Solvothermal preparation of maleic anhydride grafted onto acrylonitrile–butadiene–styrene terpolymer (ABS). Polymer 2005;46:4098–104.
[17] Qi R, Yu Q, Shen Y, Liu Q, Zhou C. Grafting copolymerization of maleic anhydride onto styrene–butadiene–styrene block copolymer through solvothermal process. J Appl Polym Sci 2006;102:5274–9.
[18] Saier E, Petrakis L, Cousins LR, Heilman WJ, Itzel JF. Infrared and nuclear magnetic resonance of maleic anhydride copolymers and their half esters. J Appl Polym Sci 1968;12:2191–200.
[19] Hasenbein N, Bauer P, Schlemmer L, Hauss AF, Gropper H, Ohlinger R. (BASF Aktiengesellschaft). US Patent 5194509, March 16, 1993.
[20] Derouet D, Phinyocheep P, Boccaccio G, Brosse JC. Synthesis of photocrosslinkable elastomers by chemical modification of liquid natural rubber. J Nat Rubber Res 1991;6:39–54.
[21] Tager A. Physical chemistry of polymers. Moscow: Mir Publishers; 1978.
[22] Shen H, Wang Y, Mai K. Effect of compatibilizers on thermal stability and mechanical properties of magnesium hydroxide filled polypropylene composites. Thermochim Acta 2009;483:36–40.
[23] Bongiovanni R, Gagnor B, Malucelli G, Priola A. Surface properties and adhesion of maleinized polyethylene films. J Mater Sci 1998;33:1461–5.
[24] Lin CW, Lee WL. An investigation on the modification of polypropylene by grafting of maleic anhydride based on the aspect of adhesion. J Appl Polym Sci 1998;70:383–7.
[25] Schultz J, Lavielle I, Carre A, Comien PJ. Surface properties and adhesion mechanisms of graft polypropylenes. J Mater Sci 1989;24:4363–9.
[26] Owens DK, Wendt RC. Estimation of the surface free energy of polymers. J Appl Polym Sci 1969;13:1741–7.
[27] Packham DE. Surface energy, surface topography and adhesion. Int J Adhes Adhes 2003;23:437–48.
[28] Basak GC, Bandyopadhyay A, Bharadwaj YK, Sabharwal S, Bhowmick AK. Adhesion of vulcanized rubber surfaces: characterization of unmodified and electron beam modified EPDM surfaces and their co-vulcanization with natural rubber. J Adhes Sci Technol 2009;23:1763–86.
[29] Comyn J, Day J, Shaw SJ. Durability of aluminium–sealent joints in jet-fuel, water and antifreeze. Int J Adhes Adhes 1997;17:213–21.
[30] Husein H, Chan C, Chu PK. Surface energy and chemistry of ethylene–propylene–diene elastomer (EPDM) treated by plasma immersion ion implantation. J Mater Sci 2002;21:1611–4.
[31] Zosel A. Adhesion and tack of polymers: influence of mechanical properties and surface tensions. Colloid Polym Sci 1985;263:541–53.
[32] Konar J, Kole S, Avasthi BN, Bhowmick AK. Wetting behavior of functionalized silicone and EPDM rubber. J Appl Polym Sci 1996;61:501–6.
[33] Babai-Cline M, Wightman JP. Surface analysis and peel strength of aged, oxygen gas plasma-modified and plasticized poly (vinyl chloride) films. Int J Adhes Adhes 1995;15:185–90.
[34] Konar J, Bhowmick AK, Mukherjee ML. Contact angle hysterisis and ESCA studies on aged polyolefins. J Surf Sci Technol 1992;8:331–42.